



# A Pilot Study of Wearable Respiratory Driven Right and Left Nostril Breathing

B. R. Purnima,<sup>1</sup> N Sriraam,<sup>2,\*</sup> T. D. Senthilkumar,<sup>1</sup> M. Pavithra,<sup>3</sup> D. Kiran<sup>4</sup> and Rajkumar Dham<sup>4</sup>

## Abstract

Analysis of breathing patterns reveals factors influencing the nasal airflow passages. Shiva Swarodaya in Swara Yoga texts emphasizes the importance of right and left nostril breathing practice. A non-invasive and wearable nasal mask that continuously monitors the breathing parameters using temperature, pressure, and humidity sensors, providing real-time data from both nostrils, has been developed. The study focuses on distinguishing airflow signals from two nostrils and classifies the individuals as active-right and active-left nostril breathing by leveraging artificial intelligence (AI)-driven machine learning classification models for the classification and prediction. The statistical features, such as mean, median, standard deviation, skewness, and kurtosis, along with Teager energy and Shannon's entropy calculated from every 30-second segment of temperature, pressure, and humidity signals collected from both nostrils, were used for classifying the breathing as active-right-nostril-breathing and active-left-nostril-breathing. k-nearest neighbors (KNN) algorithm, random forest (RF), and support vector machine (SVM: linear, polynomial, radial basis function) were evaluated using accuracy, precision, recall, and F1-score. SVM-RBF achieved the highest accuracy of 98.06, precision of 0.98, recall of 0.98, and F1-score of 0.98. Accurate nostril dominance classification aids in optimizing performance, nervous system function, and stress management. The developed algorithm revealed that right-nostril breathing increases breathing rate, tidal volume, and minute ventilation, with shorter inhalation and exhalation time. The web-app is developed for respiratory insights and vital feature predictions.

**Keywords:** Active right nostril breathing; Active left nostril breathing; Breathing rate; Swara Yoga.

Received: 11 January 2025; Revised: 10 March 2025; Accepted: 18 March 2025.

Article type: Research article.

## 1. Introduction

The study of nasal airflow signals plays a critical role in health assessment, as numerous autonomic and voluntary physiological functions are closely linked to respiration and neural components located near the base of the nose. Scientific research has shown that the reproductive, excretory, and visceral organs are connected to the nerves in the nasal mucosa. Disruptions in these organs may result from improper or irregular breathing patterns in the nostrils and conversely,

disturbances in these organs can also affect nasal breathing patterns.<sup>[1]</sup>

Regular monitoring of nasal airflow can aid in tracking the progression of respiratory illnesses such as COVID-19 and in evaluating the effectiveness of treatments. Signals from the right and left nostrils offer valuable insights into a patient's respiratory function, making them particularly useful in assessing the breathing efficiency of individuals affected by COVID-19. Understanding the dynamics of right- and left-nostril breathing may be especially relevant in managing COVID-like conditions due to its potential benefits for respiratory health, stress regulation, and overall well-being.<sup>[2]</sup> As illustrated in Fig. 1, right-nostril breathing is associated with the sympathetic nervous system, which is responsible for stimulating, energizing, and activating bodily functions. Practicing right-nostril breathing may enhance alertness and improve oxygen intake, potentially boosting respiratory efficiency and sustaining energy levels, particularly useful during periods of fatigue. In contrast, left-nostril breathing is linked to the parasympathetic nervous system, which governs relaxation, calming, and restorative processes. This mode of

<sup>1</sup> Department of Electronics and Communication Engineering, M S Ramaiah Institute of Technology, Bangalore, Karnataka, 560054, India

<sup>2</sup> Department of Medical Electronics Engineering, Dayananda Sagar College of Engineering, Bangalore, 560078, India

<sup>3</sup> Department of AIML, BNMIT, Bhageerathi Bai Narayana Rao Maanay Institute of Technology, Bangalore, 560070, India

<sup>4</sup> Atamabodh Centre for Learning and Healing, Bangalore, 560085, India

\*Email: [sriraam-ml@dayanandasagar.edu](mailto:sriraam-ml@dayanandasagar.edu) (N. Sriraam)

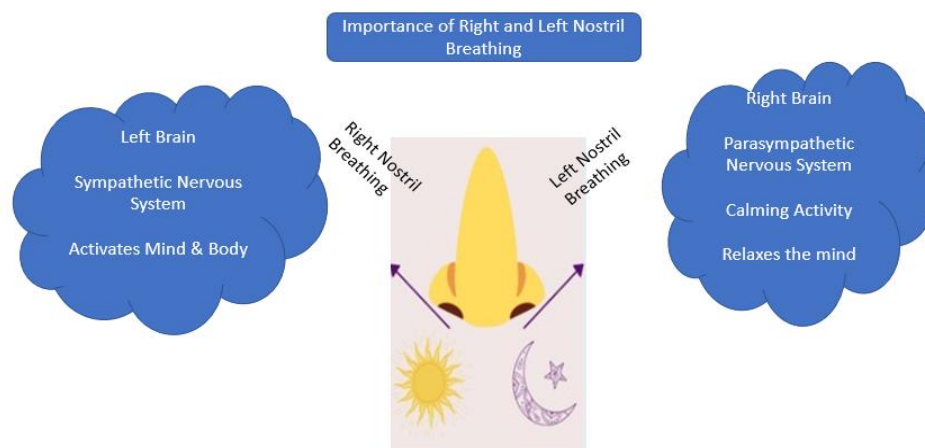


**Fig. 1:** Importance of right-nostril-breathing and left-nostril-breathing.

breathing can help alleviate stress and induce a sense of calm, which is crucial during recovery from illness.<sup>[3-5]</sup>

The natural alternation in airflow between the right-nostril and left-nostril, has long intrigued experimenters and interpreters across colorful disciplines. The assessment of individual nostril breathing plays a pivotal part in respiratory function, autonomic nervous system regulation, and overall health. Due to temporary asymmetric nasal tube occlusion by erectile tissue, it has been shown that nasal airflow in one nostril is larger than in the other.

The deep impact of breathing rhythm on emotional and cognitive processes has been known since antiquity., leading to the development of numerous breathing exercises that target mental clarity and the reduction of pain, stress, and anxiety .The breathing through left nostril alone can aid in reducing the day dreaming/mind wandering whereas right-nostril breathing has a stronger effect on wellbeing. Thus both the type of breathing are beneficial in addressing different conditions. However, they can be used to accomplish various objectives in both clinical and non-clinical groups.<sup>[6,7]</sup> The significance of active right or active left nostril breathing was very well known in Swara Yoga, thousands of years back by Shiva Swarodaya.As per the Swara Yoga the nose is considered the opening to inner-world. The nose is essential for breathing, prana absorption, and energy circulation. It is a crucial point where energy from the outside and within worlds is communicated. The brain and energy circuits get impulses from tiny nerve detectors located at the membrane of the nose when the outside air comes into touch with the nasal passages.Thus, by controlling the breath that enters and exits through the nose, swara yoga teaches us to master the inner body mechanism and to obtain complete control over all pranic (energy) and mental activity.

Swara Yoga as given in the Shiva Swarodaya talks about the three energy flow circuits related with the active nostril air flow -left nostril, or right nostril, and when both left and right nostrils are active. The energy flows through Nadis (nadi in yoga, which is a channel of flow of energy and doesn't have any physical existence. When the airflow is more in the left-

nostril, Chandra-nadi is active and when the airflow is more in the right nostril, Suryanadi is active. Swara yoga emphasizes that by using a particular breathing technique, one may regulate and manage the two main energy circuits, Surya and Chandra.<sup>[8]</sup> The proposed yoga philosophy further indicates that any disruption in the energy circuits can have an impact on breathing.

The two energy circuits operate in varying sequences and flow in the rhythmic cycle in swara yoga.<sup>[8]</sup> Further practices of single nostril yoga breathing seem to have varying effects on blood pressure. Active-right-nostril-breathing is a breathing exercise where one inhales and exhales only through the right nostrils, often referred to as Surya Bhedana, and it is allied with stimulating the energy of the body, plus increasing alertness. The practice is believed to activate the body's energy channels and is associated with several benefits. Active left nostril breathing is a technique that emphasizes inhalation and exhalation through the left nostrils, referred to as Chandra bedana, and its practice is believed to have calming effects and be a beneficial addition to our daily routine, helping to promote relaxation, emotional balance, and overall well-being.<sup>[9-12]</sup> Thus, different physiological effects of right and left single nostril breathing and Alternate-nostril breathing techniques align with the traditional swara yoga concept that the air flow through the right nostril is activatory in nature, while the air flow in the left nostril is relaxatory in nature.<sup>[13]</sup> The autonomic nerve system is directly impacted by right, left, and alternate nostril yoga breathing. This effect can be measured by skin conductance, blood pressure, finger plethysmogram amplitude, heart rate variability analysis, and skin conductance. Diastolic and systolic pressures rise significantly with active breathing via the right nostril, while they fall with active breathing through the left nostril.<sup>[14]</sup> These outcomes raise the possibility of therapeutic uses.

Closing one nostril with the right-thumb and then exhaling through the other is one method to initiate right or left nostril breathing. Repeat this process until the desired number of breaths is taken. Nasal visualization, or mentally concentrating on breathing through one nostril and influencing the body to

favor that nostril, is another way to engage the nostrils without physically closing them. This technique is achievable for yoga practitioners who are familiar with Swara yoga practice.

The evaluation of distinct nasal breathing was made possible by using various discrete and advanced measurement techniques that have evolved with technology. The difference in the airflow from the nostril during breathing may be observed qualitatively by placing the hand vertically in the middle of the face with the fingers facing up, touching the midline of the nose, and breathing, noting a clear difference in airflow as we exhale. Quantitative measurement of nasal airflow signals has evolved over the years with the advent of technology. Techniques like rhino-resistometry, rhino-manometry, acoustic-rhinometry, flexible-liquid-crystal thermography, and Magnetic Resonance Imaging-structural imaging of the turbinate are a few of the developments that contribute to nasal cycle analysis, with the limitation of not being translated to a wearable setting mode.<sup>[15]</sup> The advent of small thermal sensors, auditory sensors, and pressure sensors for capturing the nasal airflow signals by placing the sensors near the nostrils using cannula has paved the way to arrive at wearable tools for the measurement of breath signals. Roni Kahana-Zweig *et al.*<sup>[16]</sup> used a readily available cannula with separated tubes for each nostril connected to a compact wearable-device.

In order to gather dual nostril airflow signals, the gadget has two high-sensitivity pressure sensors that were coupled to a data logger to enable lengthy hours of continuous recording.<sup>[16]</sup> Niazi *et al.* determined how unilateral Yogi nasal breathing altered the encephalographic (EEG) signals. Through the manipulation of nasal airflow and the observation of brain activity patterns through EEG recordings, they investigated the relationship between sympathetic and parasympathetic activity and breathing through the right and left nostril. It has been noted that the airflow via the left and right nostrils appears to affect brain functions differently.<sup>[17]</sup> Sinha *et al.* (2021) assessed the effect of individual nostril breathing on lung function parameters and heart rate during resting condition. They performed a study on 35 healthy volunteers of 18-40 years of age group. The participants were characterized into right nostril dominance group and left nostril dominance by subjecting them to cold mirror test. Using a pulse oximeter, Using the SPSS tool, they analyzed various pulmonary function parameters and was noticed that they exhibited higher values in Right-Nostril-Dominant Breathing participants compared to Left-Nostril-Dominant-Breathing participants and attained a good statistical significance of  $p < 0.5$ .<sup>[18]</sup>

In recent years, numerous researchers have developed respiratory monitoring devices using various sensors, diverging from traditional dual nostril breathing assessment methods. A comprehensive overview of wearable and remote respiratory monitoring devices is provided in.<sup>[19]</sup> For instance, Chu *et al.* created wearable strain sensors to measure respiration rate and volume, consisting of a piezoresistive

metal thin film embedded in a silicone elastomer substrate.<sup>[20]</sup> In 2023, Hossein Cheraghi Bidsorkhi and colleagues designed a Smart face mask by applying graphene-based coatings to commercial surgical masks, specifically incorporating graphene nanoplatelets (GNPs) into a polycaprolactone (PCL) polymeric matrix. They also developed a mobile application to alert users of cough and dyspnea, although signal acquisition was limited to single nostril breathing and few respiratory vital calculations were performed.<sup>[21]</sup> That same year, Zhang *et al.* engineered a system comprising a triboelectric respiratory sensor with a hardware circuit board for data acquisition, pre-processing, and wireless transmission. Their system included a machine learning algorithm to enhance recognition accuracy and a mobile terminal app. The triboelectric sensor, fabricated using the screen-printing method, was lightweight, non-invasive, and biocompatible. The self-built circuit board collected and pre-processed five typical respiratory behaviors (normal breathing, deep breathing, sneezing, coughing, and laughing) through filtering and smoothing techniques.<sup>[22]</sup>

The existing literature suggests that real-time monitoring of airflow patterns helps healthcare professionals identify various abnormalities, including nasal congestion, septal deviations, and nasal cycle disturbances. This has broad applications in clinical settings, sports performance, and stress management. There is an ongoing need to detect and analyze nasal airflow patterns and durations, as these contribute to diagnosing physiological and psychological changes in humans. Additionally, this information holds significant importance in traditional medicine systems such as Siddha, Ayurveda, and Yoga. The current research indicates a lack of development in wearable devices for assessing individual nostril breathing patterns and characterization of breathing patterns through respiratory vitals. Therefore, the proposed study aims to address these research gaps in the field of wearable respiratory assessment.

The subsequent points are the major contributions of the proposed work:

1. A smart wearable electronic mask with flexible electronics is fabricated allowing continuous measurement and recording of temperature, pressure, and humidity variations in each nostril separately.
2. Using a wearable electronic mask that captures temperature, pressure and humidity variations developed at Ramaiah Institute of Technology, a cohort of data consisting  $n=15$  with 15-minute recording with two trials was created from yoga practitioners of Atamabodh Centre for learning and healing, Bangalore, India.
3. By oversampling the minority class, the synthetic-minority-over-sampling technique (SMOTE) was used to address class imbalance.
4. Identification of the difference in the airflow signals from left and right nostrils was attained.

5. Different Machine learning models were explored for effective classification of active right or active left nostril patterns (*i.e.*, left or right) based on the collected environmental data. A robust support vector machine (SVM) classifier model with radial basis function (RBF) kernel was developed for the classification with highest accuracy of 98.06%, precision of 0.98, recall of 0.98, and F1-score of 0.98.

6. Prediction of right/left nostril breathing using the nasal airflow signals was acquired

7. Categorized breathing into two types: active-right-nostril breathing and Active-Left-Nostril-Breathing and examined how these breathing patterns impact human health by utilizing advanced technologies to predict the type of breathing.

8. Comprehensive solution to analyze breathing data efficiently is offered by deriving meaningful insights into respiratory vitals such as breathing-rate, inhalation-time, exhalation-time, inter-breath-intervals, and tidal volume rate, minute ventilation from the acquired breath signals which confirms the variations between the two categories considered.

9. Robustness and real-world relevance of the developed Breathing metrics prediction system is showcased with a Web application that presents the prediction of active right/left nostril breathing and displays the values of respiratory vitals.

The organization of the manuscript is as follows: Section 2 provides the materials and methods with a clear description of the overall framework, data collection procedure, data cleaning methods, information of respiratory vitals calculated, classification and prediction methods incorporated, and the details of front-end application programming interface (API) development. Section 3 presents the experimental results, including raw data plots, results of the data cleaning process, results of exploratory data analysis, and performance

evaluation metrics of classification and prediction models. A comparison of respiratory vitals among the active right nostril and active left nostril breathing is given, and a front-end API to display the prediction results and respiratory vitals. Additionally, section 3 compares cutting-edge methods in the suggested context and displays the main findings of the suggested investigation. Finally, the concluding remarks in section 4 signify the importance of the proposed study.

## 2. Methodology

### 2.1 Overall framework

Fig. 2 presents the overall framework of the current study. The data acquisition was performed using a wearable nasal mask, having a BME280 sensor with an ESP32 microcontroller, developed at Ramaiah Institute of Technology, Bangalore, India. The wearable nasal mask was designed to capture the temperature, pressure, and Humidity variations at both nostrils. The raw data was cleaned for the removal of outliers, non-integer values, and empty space caused during the acquisition process, and it was detrended for the removal of baseline drift in the signal. To preserve the stationarity, the data was cleaned and segmented with a window size of 30s, and the selected features like Teager energy, Shannon entropy, and statistical features like kurtosis, skewness, and std. deviation, mean, and median were extracted from each segment. To classify the respiratory data into active right or active left nostril breathing, the extracted features were grouped into training and test set data in the ratio (80-20) and subjected to machine learning model that yielded very good accuracy in classification and the details of machine learning model deployed in this study has been reported in section 3.

Further, in order to characterize the breathing status of all the participants, the cleaned data was used to calculate respiratory vitals like breathing-rate, inter-breath interval, inhalation-time, exhalation-time, tidal volume, and minute

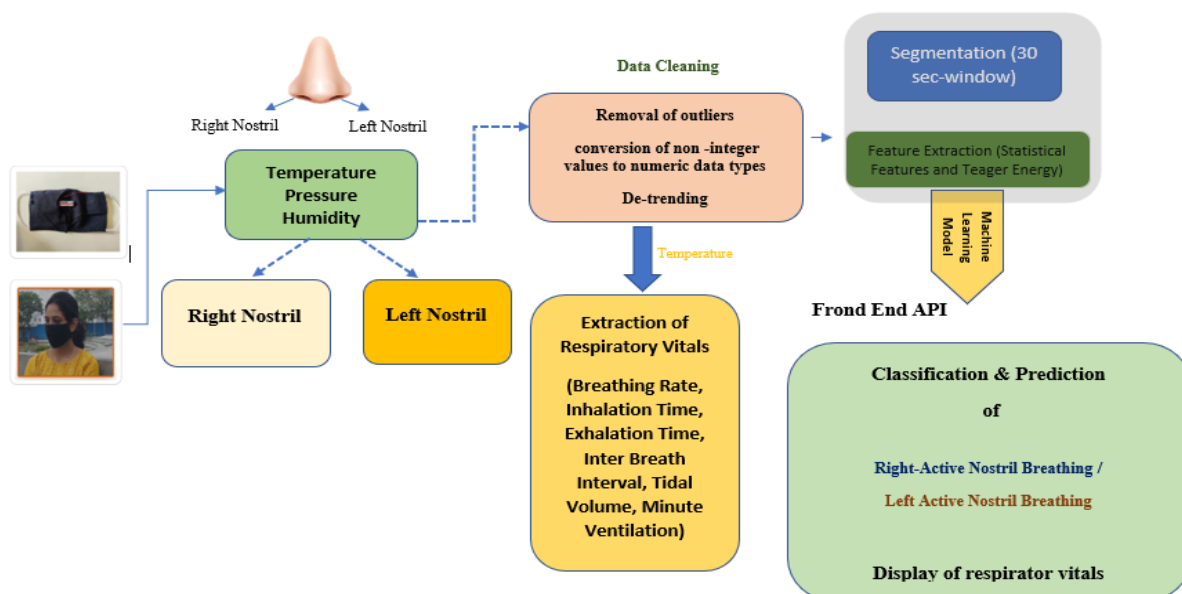


Fig. 2: Proposed framework for breathing assessment through wearable nasal sensing mechanism.

ventilation by using the developed customized algorithm on an open-source platform. A front-end API was developed to visualize the results of classification and prediction of active-right or active-left nostril breathing and display of respiratory vitals.

## 2.2 Data collection

The breathing data from both the nostrils was acquired using a wearable nasal mask, developed using BME280 sensor. This entails the integration of miniature sensors for temperature, pressure and humidity sensing into a comfortable and user-friendly wearable device. The prototype is capable of capturing real-time nasal parameter data with high accuracy and reliability, laying the foundation for subsequent research and clinical applications. The ethics approval for the usage of the developed device was obtained from Ramaiah Medical College and Hospitals, Bangalore, India. These sensors were strategically positioned within the mask to come into direct contact with the nasal environment, allowing accurate and sensitive data capture. Careful consideration was given to sensor placement to ensure optimal sensing performance and user comfort during wear.

A pilot study was done on 15 healthy yoga practitioners of 30-50 years of age group at Atamabodh Center for Learning and Healing, Bangalore. They master the practice of Swara Yoga, which is a style of yoga that places a strong emphasis on studying, managing, and adjusting breath as a way to reach self-realization. It is an ancient tantric science that involves the systemic study of breath through the nostrils.<sup>[23]</sup> The yoga practitioners at Atamabodh Centre for Learning & Healing are proficient in understanding their breathing status and control the breathing as per the need. *i.e.*, they are trained to alter the individual nostril breathing. They are experts in activating single-nostril breathing, during which the respective nostril is expected to have free airflow without any obstruction. The yoga practitioners were made to sit in a relaxed state and wear the mask, ensuring a secure and comfortable fit and were asked to focus on which nostril they are active in. Based on their response, the participants were grouped into Active-Right-nostril-Breathing and Active-Left-nostril-Breathing groups. With clear instructions to participants regarding the proper wearing and maintenance of the mask during the data collection period, breathing patterns were recorded, and a cohort of 30 samples was created, having breathing signals for two trials from two groups labelled as Active right-nostril-breathing and Active-left-nostril-breathing groups. A database of 15-minute recordings from 15 volunteers by 2 trials was created by taking consent from all the subjects. Participants were encouraged to provide feedback on their wearing experience, including any discomfort or issues encountered during data collection. By adhering to standardized protocols and best practices, we collected high-quality and reliable data that formed the foundation for subsequent analysis and modelling. The raw breathing data is stored in a structured file,

txt format, preserving the temporal sequence of observations and associated sensor readings.

## 2.3 Data cleaning

Data preprocessing was of paramount importance in the current study, as it ensures the quality, reliability, and usability of the collected data for subsequent analysis and modelling. By employing rigorous preprocessing techniques and best practices, we unlock the full potential of the data, leading to accurate predictions, valuable insights, and advancements in nasal health monitoring and management. The collected data was inspected for completeness, accuracy, and potential issues such as sensor malfunction or data corruption. Missing values in the dataset, if any, were identified and addressed using appropriate techniques such as imputation. To ensure consistency in data representation and compatibility with machine learning algorithms, the data types of relevant features were checked and converted to a numeric format if necessary. Outliers were identified and removed to prevent them from skewing the analysis or model training using the interquartile range (IQR). The data was further subjected to detrending and normalization for further analysis.

## 2.4 Extraction of respiratory vitals

This section presents the implementation of algorithms to derive respiratory vitals from the captured nasal parameter data. Using the cleaned data, the respiratory vitals like breathing rate, inter-breath intervals, tidal volume, and minute ventilation were acquired using the developed algorithm on an open-source platform. The algorithm uses the temperature signals of the breathing data captured from multiple sensors that include temperature, pressure, and humidity sensors. It provides a comprehensive toolkit for processing and analyzing respiratory data to monitor respiratory health and performance. Below are the definitions of the extracted respiratory vitals.

**Breathing Rate:** The number of inhalation and exhalation cycles per minute (breaths/min).

**Inhale Inter-Breath-Interval:** The typical duration (in seconds) between every two inhalation peaks for each sensor.

**Exhale Inter-Breath-Interval:** The typical duration (in seconds) between every two exhalation peaks for each sensor

**Inter-breath-Interval:** The time in seconds between every two exhalation peaks for each sensor.

**Tidal Volume Rate:** The quantity of air measured in millilitres taken in or out per breath for each sensor

**Minute Ventilation:** The total quantity of air measured in milliliters taken in or out per minute for each sensor

## 2.5 Classification and prediction of active right/ left nostril breathing

The exploration of active nostril breathing has the potential to clarify important facets of human behavior and health, and the traditional methods of assessing individual nostril breathing have relied largely on subjective observation and rudimentary measurement techniques. However, with recent advancements

in sensor technology and machine learning, there arises an exciting opportunity to revolutionize the study of active nostril breathing and its implications. Machine learning models are crucial components of this work, tasked with analyzing environmental data captured by nasal mask sensors to predict active-right-nostril-breathing or active-left-nostril-breathing. This study focused on classifying and predicting active-right or active-left-nostril breathing based on nasal airflow signals, acquired using a wearable mask developed with a BME280 sensor. The flowchart of the proposed classification and model for prediction is shown in Fig. 3.

The flowchart represents the process of classifying respiratory signals from the right and left nostrils in the active right nostril breathing and active left nostril breathing groups. Fig 3a shows that the raw respiratory signals undergo a data

cleaning process, where outliers are removed, and non-integer values are converted to integers. The cleaned data is then segmented into 30-second intervals, and feature extraction is performed on each segment. Fig. 3b shows that the extracted features serve as inputs to various classification models, including k-nearest neighbors (KNN), random forest (RF), and SVM with different kernels. The best classification model is determined using a performance evaluation matrix, which assesses accuracy and effectiveness. Among the tested models, SVM with an RBF kernel demonstrated the highest accuracy in distinguishing between active right nostril breathing and active left nostril breathing groups.

The developed model is supervised as it is trained on labelled data containing environmental parameters from nasal mask sensors and corresponding labels indicating the nature

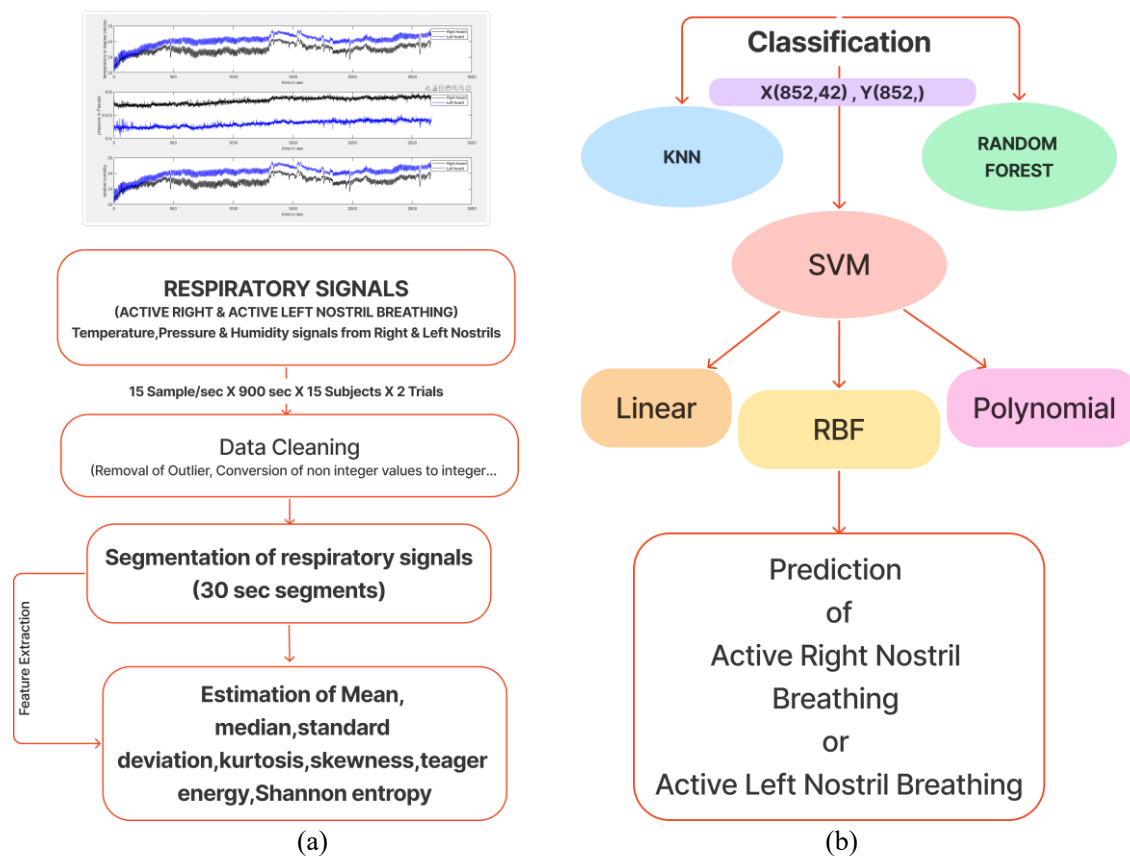


Fig. 3: Flow chart for classification and prediction active right or active left nostril breathing.

of breathing as Active-right or Active-Left nostrils. Key steps in the development of this model include data cleaning, model training, evaluation, and refinement. The cleaned data containing temperature, pressure, and humidity variations of right and left nostrils was segmented with a segment size of 30 sec without overlap, and features like Teager energy, Shannon entropy, mean, median, kurtosis and standard deviation were obtained from each segment as input and the target variable was set as the active-right or active-left-nostril-breathing for the model development. The Teager energy operator (TEO) is a nonlinear operator used in signal processing to measure the energy of a signal. It is particularly effective for analyzing the

instantaneous energy of a signal, which can provide insights into its frequency and amplitude variations over time.

For a discrete-time signal  $x_1(n)$ , the Teager energy operator  $\phi_1$  is defined by Equation (1).<sup>[24]</sup>

$$\phi_1\{x_1(n)\} = x_1(n)^2 - x_1(n-1) * x_1(n+1) \quad (1)$$

Shannon developed the idea of Shannon entropy ( $S_1$ ), which measures the quantity of information in physical systems. It is calculated using Equation (2) (Shannon, 1948).<sup>[25]</sup>

$$S_1 = \sum_{i=1}^p k_i \log_2 \frac{1}{k_i} \quad (2)$$

where  $p$  is the total number and  $k_i$  is the probability of the situation  $i$  in the system.

In order to handle class imbalance by oversampling, synthetic-minority-over-sampling-technique was used to create sets for training and testing from datasets. Given the minimal data size and ethical considerations, a machine-learning approach was adopted instead of a deep learning approach. The selection of an efficient model was done by comparing the results of KNN, RF and SVM-Linear, Polynomial and RBF kernels.

**2.5.1 KNN classifier**

The task of classification was initiated with the use of a simple but powerful nonparametric method, the KNN algorithm. The KNN classifier with  $K=5$  was employed to classify Active-right and Active-left-nostril-breathing categories. The classification of a new data point was done based on the majority class among its 5 nearest neighbors in the feature space. After empirical testing with cross-validation,  $K=5$  was chosen as it provided an optimal balance between bias and variance, yielding perfect accuracy on the validation set. The Euclidean distance was used as the distance metric for identifying the nearest neighbors due to its simplicity and effectiveness. Its performance highlights the importance of careful selection of the  $K$ -value to balance the trade-off between overfitting and underfitting.

**2.5.2 RF classifier**

Another Robust, versatile classifier with strong performance is an RF classifier, which is used for a variety of applications. It is an ensemble-learning method that operates by building a multitude of decision trees during training and outputs the mode of the classes or the mean prediction of the individual trees. The core idea behind the RF algorithm is the use of multiple decision trees, where each tree is trained on a random subset of the data (bagging). Each tree in the forest is built using a random selection of features, which introduces variability and ensures that each tree is unique. This randomness helps prevent overfitting, a common problem in decision trees, especially when the dataset is noisy or has high

dimensionality.<sup>[26,27]</sup> Among the classifiers like KNN and other single decision tree models, RF is a robust model as it reduces overfitting. Further, it is less sensitive to noise and outliers, making it a more stable choice.

**2.5.3 SVM Classifier**

SVM is a resourceful and influential model for the classification of categories, capable of handling both linear and non-linear data through the use of a variety of kernel functions. One of the suitable models for the classification and regression tasks is the SVM, which is a prevailing supervised learning model. In this study, we employed an SVM-Linear kernel, Polynomial kernel, and a RBF kernel to classify Active-right-nostril-breathing and Active left-nostril-breathing signals. The model development was performed using the Scikit-learn library. The model was trained with the selected parameters on the training dataset, and its performance was evaluated on the test set.<sup>[28]</sup> The construction of the SVM with RBF is demonstrated in the following Fig. 4.

(1) Linear-kernel

The inner product (dot-product) between any two vectors in the original feature space is computed by using the linear-kernel. The decision function for a linear-SVM can be expressed as shown in Equation (3):

$$f(y) = \omega_1 \cdot y + c \tag{3}$$

where  $y$  is the input feature vector,  $\omega_1$  is the weight vector, and  $c$  is the intercept, which shifts the decision boundary.

The decision boundary is a hyperplane defined as Equation (4):

$$\omega_1 \cdot y + c = 0 \tag{4}$$

The classification of data points is either towards  $f(y) > 0$ , or  $f(y) < 0$ , depending on which side the hyper-plane falls.

(2) Polynomial kernel

Another SVM kernel used to capture complex and nonlinear relationships within the data is polynomial kernel. It was selected due to its ability to model interactions between features that cannot be captured by a simple linear boundary. The polynomial kernel allows the SVM to construct a decision boundary by transforming the original feature space into a

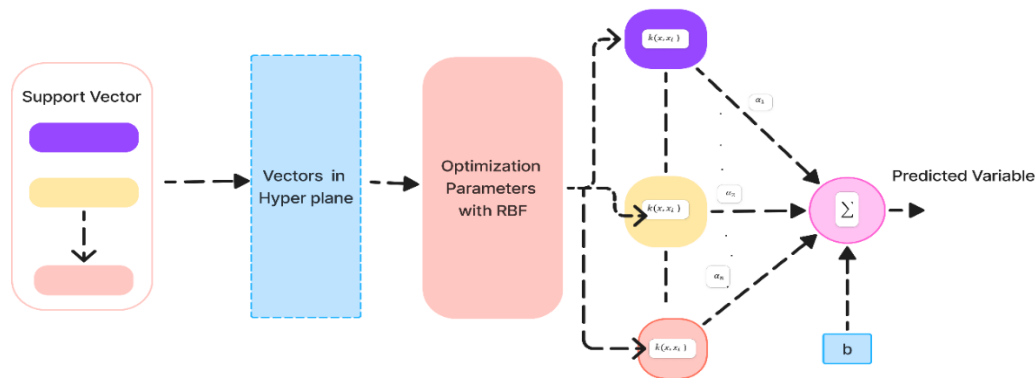


Fig. 4: Construction of SVM model with RBF kernel.

higher-dimensional space, helping to effectively separate classes that are non-linearly separable in the original space. The polynomial kernel is defined as given in Equation (5):

$$M(y_i, y_j) = (z \cdot y_i^T y_j + r)^e \quad (5)$$

where  $z$  is a scaling factor for the input features,  $r$  is a constant term that controls the flexibility of the decision boundary, and  $e$  is the degree of the polynomial.

### (3) RBF kernel

When there is no linear separation between the features, the RBF kernel, sometimes referred to as the Gaussian kernel, is a common option for SVMs. The RBF kernel maps the input space into a higher-dimensional space, allowing the SVM to create a more flexible decision boundary that can better separate classes with non-linear boundaries. The RBF kernel is particularly effective when there is no prior knowledge of the data's distribution, as it can handle a wide variety of patterns. The mathematical formulation of RBF kernel is given in Equation (6):

$$K(y_i, y_j) = \exp(-z \cdot \|y_i - y_j\|^2) \quad (6)$$

The influence of single training example is determined by the parameter  $z$ . A smaller  $z$  smoothens the decision boundary and a larger  $z$  leads more complex model. The performance of the SVM-RBF kernel is highly sensitive to the choice of the  $z$  parameter and the regularization parameter  $C$ . The width of the Gaussian function is controlled by the  $z$  parameter. Through cross-validation, we selected the optimal values for  $z=0.1$  and  $C=1$ . These parameters were chosen to maximize classification accuracy on the validation set, balancing the trade-off between model complexity and generalization. By applying optimal hyper-parameters, the model training was performed on the dataset. The margins between the support vectors of different classes were optimized in order to train and fit SVM model to the data.

## 2.6 Frontend API development

The frontend API development encompasses the creation of a user-friendly interface through which users can interact with the predictive models and receive real-time predictions based on environmental data input. The interface enables the users to input environmental data such as temperature, pressure, and humidity for both the right and left nostrils. Upon receiving user input, the API triggers the predictive models to generate real-time predictions regarding Active-right or Active-left-nostril-breathing. The API displays the predictions in a clear and visually appealing manner, providing users with immediate feedback on which nostril they are active in. To enhance user understanding, the API includes visualizations of the predicted results, such as color-coded indicators for active

nostrils. In addition to visual representations, the API provides detailed output regarding the predicted physiological parameters associated with each nostril, such as breathing rate, inter-breath intervals, inhalation time, exhalation time, tidal volume, and minute ventilation. The frontend API ensures good screen sizes and ensures a seamless user experience, whether accessed from desktops, laptops, tablets, or smartphones.

## 3. Results and discussion

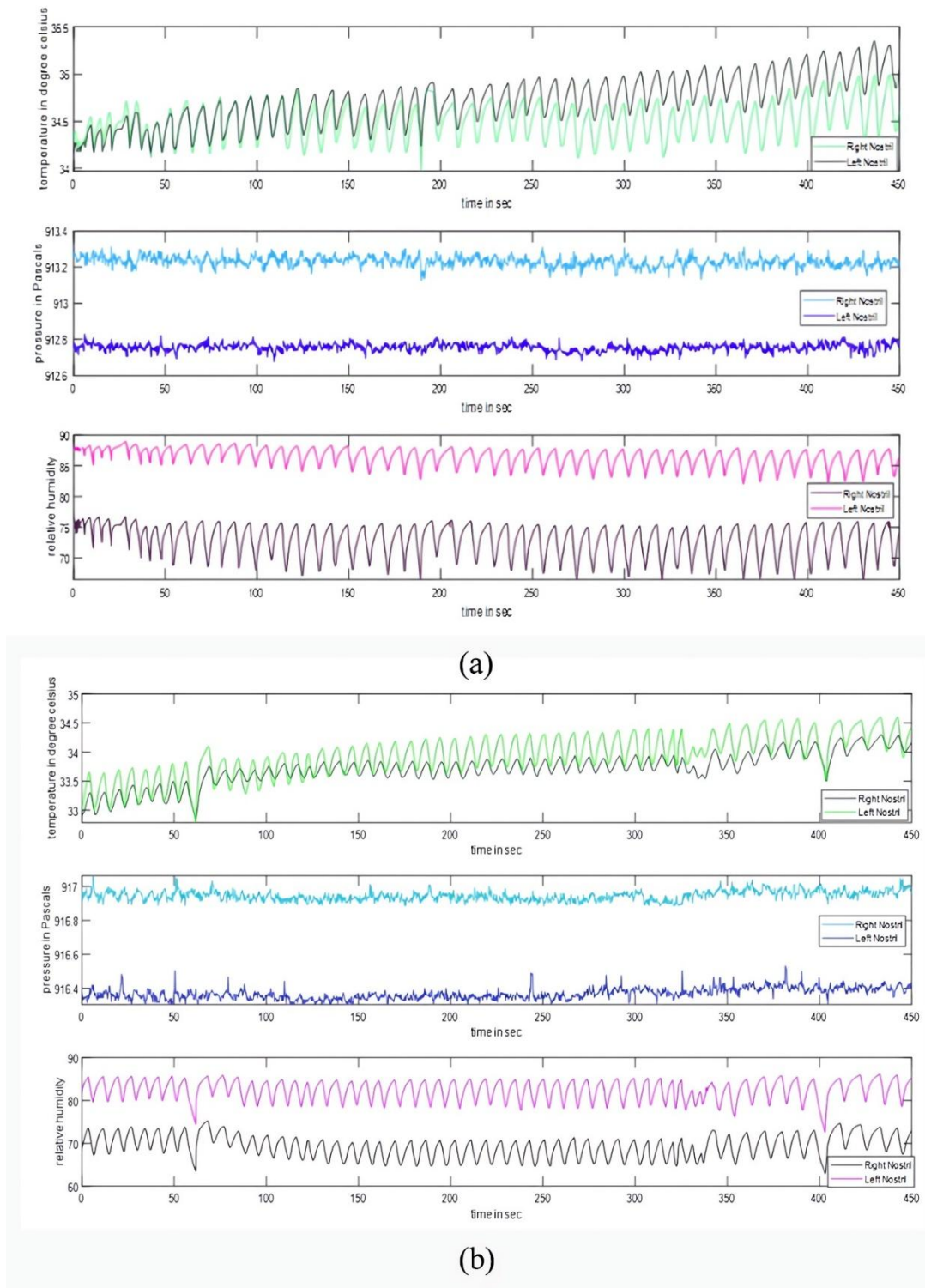
### 3.1 Raw plots

Fig. 5 shows the raw signals representing the temperature, pressure, and humidity variations from the right and left nostrils captured using the wearable nasal mask developed at Ramaiah Institute of Technology, Bangalore, India. The plots show an 8-minute recording of normal breathing signals acquired in a relaxed sitting posture from the categorized-active-right-nostril group in Fig. 5a and active-left-nostril group in Fig. 5b. Plots clearly indicate that the values produced by the right and left nostrils differ noticeably from one another in both groups. It is also evident that all the variables in the raw data are bound to have a few values out of their respective ranges, which are considered outliers. Hence, the raw data was further subjected to a data cleaning process where the outliers were removed, as shown in Figs. 6 and 7.

Fig 5a shows the raw data plot of 8 min recording of respiratory signals captured using a wearable nasal mask showing temperature, pressure, and humidity variations from active right nostril breathing group and Fig. 5b shows the raw data plot of 8 min recording of respiratory signals captured using a wearable nasal mask showing temperature, pressure, and humidity variations from active left nostril breathing group. The plots make it evident that the right and left nostrils vary significantly in terms of temperature, pressure, and humidity variables with respect to each other and also among the two groups considered.

### 3.2 Data cleaning

The raw data captured using sensors were scrutinized for missing values, which could disrupt subsequent analyses. Techniques such as interpolation or removal of incomplete data points were applied to mitigate the impact of missingness. Outliers, or aberrant data points, were identified and removed using the interquartile range (IQR) method to prevent their undue influence on analysis outcomes. Thus, the sensor data was initially cleaned for handling missing values, converting data types, eliminating outliers, detrending, and standardizing features. Fig. 6 demonstrates the Box plots to visualize the distribution of numerical columns and identify potential outliers of raw data and the Box plots of temperature, pressure and humidity signals of right and left nostrils with Outliers removed using the IQR method to improve the dataset's quality. It is observed that the potential outliers present in the raw data during the data acquisition process for all the measured variables were removed by the implementation of IQR



**Fig. 5:** a) Raw respiratory signals from active right nostril breathing group, b) Raw respiratory signals from active left nostril breathing group.

methods, and the data having temperature, pressure, and humidity values were brought to their respective limits

### 3.3 Exploratory data analysis

Across different groups (Active-right /Active-left-nostril-breathing). Each subplot figure displays a boxplot showing the distribution of right nostril temperature/pressure/humidity

values across two groups. The y-axis represents the temperature/pressure/humidity values, and the x-axis denotes the groups to be classified (Active right/Active Left Nostril breathing). Each boxplot allows comparison of physiological measures (temperature, pressure, humidity) between Active-right and Active-left-nostril-breathing. The median differences in the graph enable a comprehensive assessment of

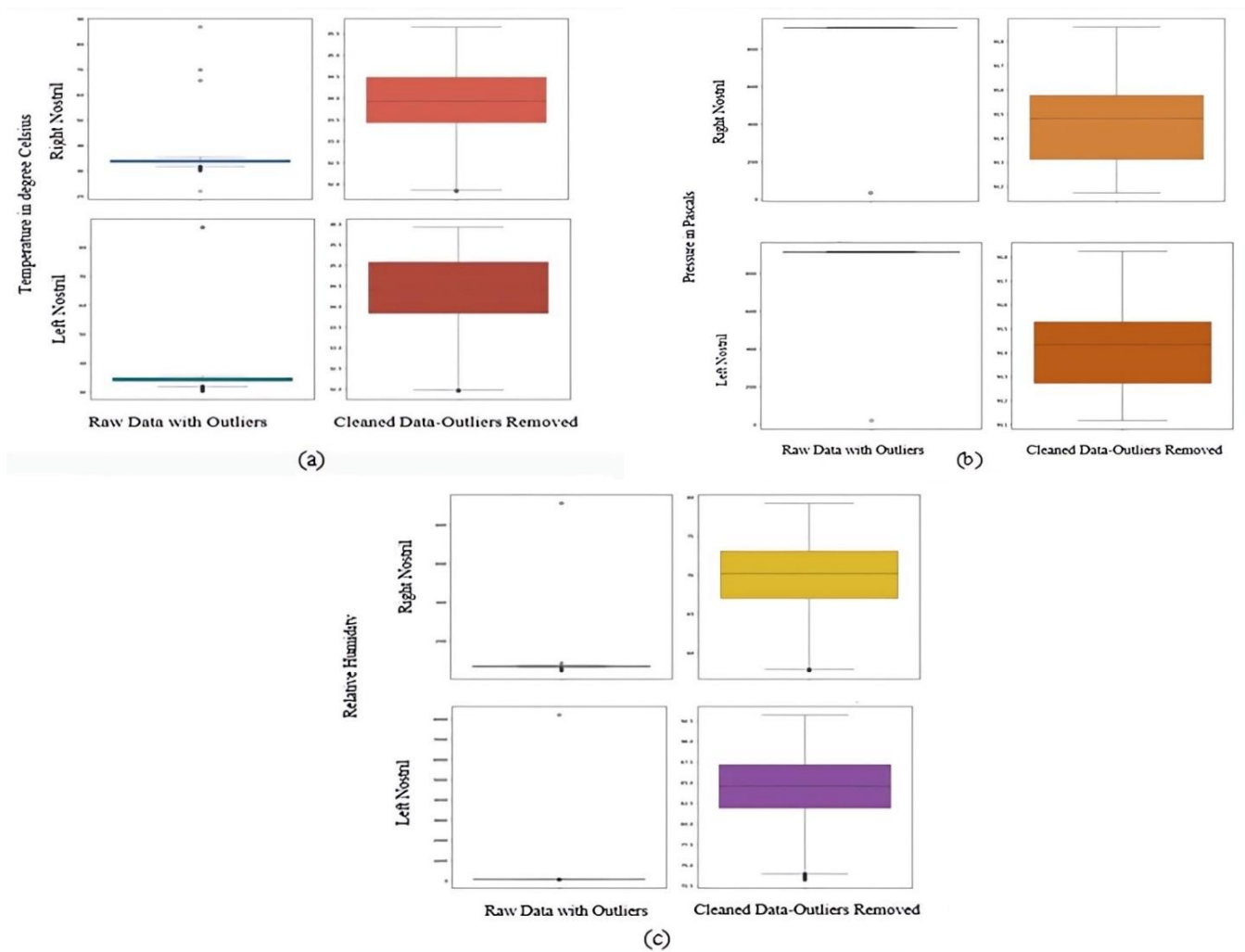


**Fig. 6:** a) Box plots to visualize the distribution of numerical columns and identify potential outliers of raw data showing temperature signals and the Box plots with outliers removed using the interquartile range (IQR) method to improve the dataset's quality, b) Box plots to visualize the distribution of numerical columns and identify potential outliers of raw data showing pressure signals and the box plots with outliers removed using the IQR method to improve the dataset's quality, c) Box plots to visualize the distribution of numerical columns and identify potential outliers of raw data showing humidity signals and the box plots with outliers removed using the IQR method to improve the dataset's quality.

how different physiological measures vary about both groups, offering valuable insights into potential asymmetries in breathing-related data across different nostril usage scenarios and paving the way for pattern classification with the highest accuracy.

Fig. 7 consists of 6 subplots, with each subplot corresponding to a specific physiological measure (temperature, pressure, humidity) for either the Active-right or Active-left-nostril-breathing. A significant difference in the median values among the two groups is observed for all the measures obtained from the right and left nostrils, contributing to the exploration of respiratory dynamics and pattern classification protocols.

### 3.4 Classification results

The input to the model was the statistical features, teager energy, and shannon entropy from 30-second segments of respiratory signals from right and left nostrils. The visual

representation that displays the significance of different features in a model developed is depicted in Fig. 8.

It is evident from the graph that the statistical features from pressure signals have the highest influence on the model's predictions. In the current study, we compared the performance of KNN, RF, and SVM with various kernels in order to develop a robust model for the classification and prediction of active right nostril and active left nostril dominant groups.

The KNN model demonstrated strong performance with an overall accuracy of 95%. The precision and recall values indicate that the model is particularly effective in correctly identifying the correct category, with a perfect precision of 1.00 for category L-active left nostril breathing and a perfect recall of 1.00 for category R-active right nostril breathing. The weighted average F1-score of 0.95 reflects the model's balanced performance across both classes. This highlights the effectiveness of KNN with careful selection of the K

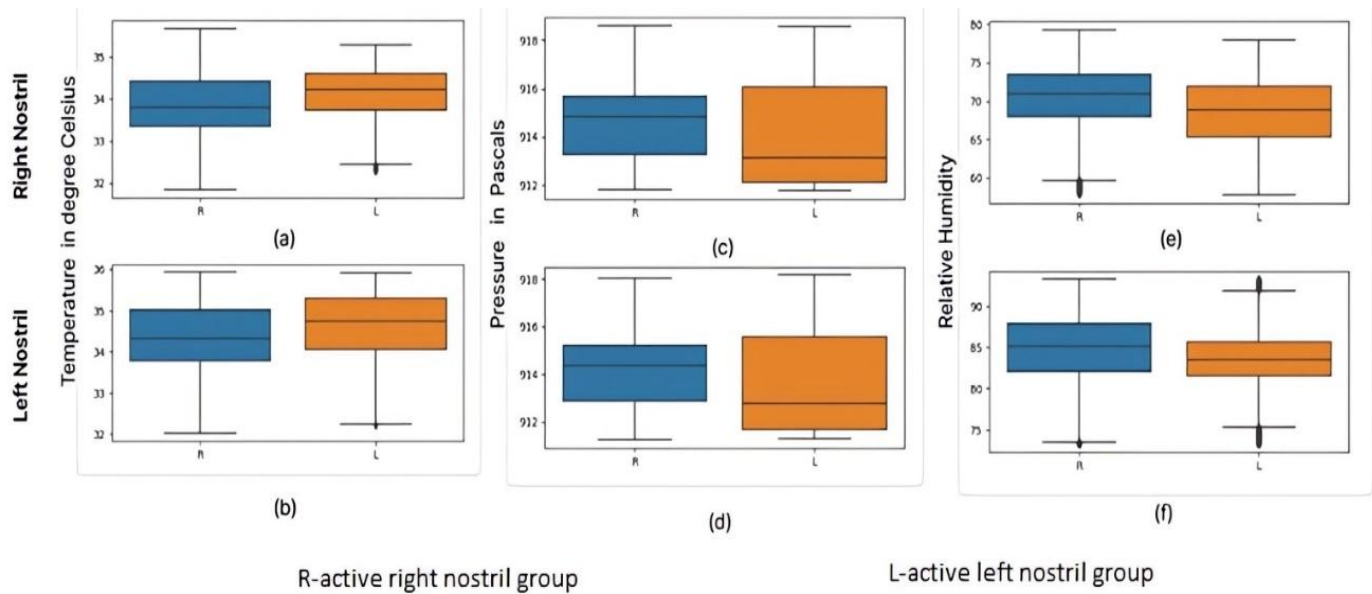


**Fig. 7:** Boxplots showing the median differences in(a,b): Temperature,(c,d): Pressure and (e,f): Humidity signals from both nostrils among two classes (R: Active Right Nostril Breathing and L: Active Left Nostril Breathing).

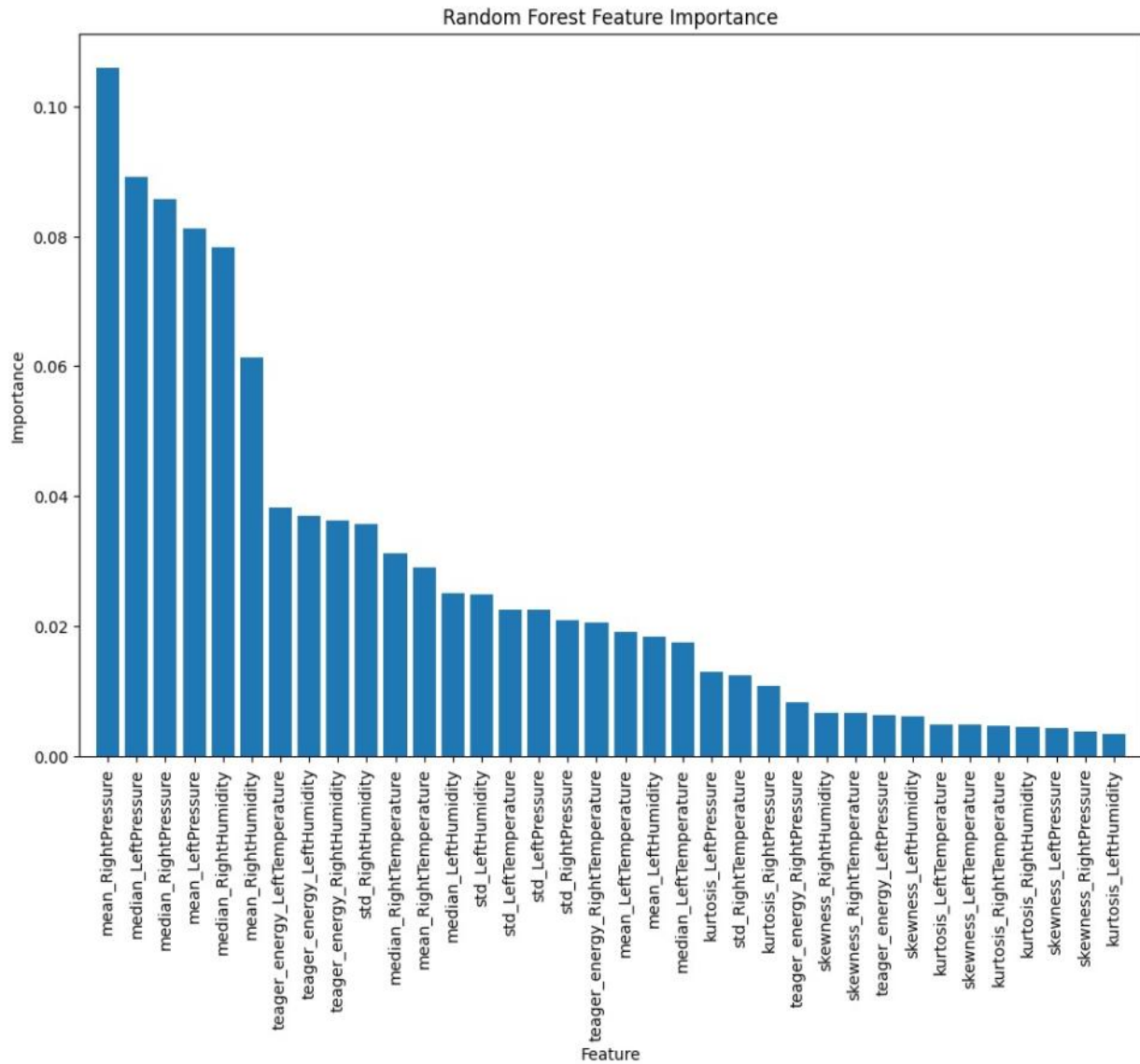


**Fig. 8:** Feature importance for the classification and prediction of active right and active left Nostril breathing.

parameter in this nostril dominance classification task.

The RF model also achieved a high accuracy of 95%, comparable to KNN. It shows a strong precision and recall for both categories, with particularly high precision for category L (0.99) and excellent recall for category R (0.98). The weighted average F1-score of 0.96 reflects the model's robustness and balanced performance, further underscoring its effectiveness in nostril dominance classification tasks.

The SVM classifier with a linear kernel did not show high accuracy, as the nature of the data was not linearly separable. When the input features and the target variables are linearly related, then a linear kernel is particularly effective. The linear SVM demonstrated average performance on the test set, achieving an accuracy of 78.06 %. The model was not effective in separating the classes, hence, SVM with linear kernel was not considered for the prediction model. The evaluation metrics like precision, recall, and F1-score metrics indicated that the model was not as effective in classifying the categories, particularly struggling with precision for category R (0.63). This performance highlights the limitations of using a linear kernel for data that is not linearly separable.

In our study, we selected a polynomial kernel with degree  $d=6$  after cross-validation indicated that this degree provided the best performance on the validation set. The choice of kernel parameters  $z$ ,  $r$ , and  $e$  was critical for achieving optimal performance. Through extensive hyperparameter tuning, the parameters were set to degree = 6, coef = 2, and  $C = 1$ . The model was trained with the selected parameters on the training dataset, and its performance was evaluated on the test set. The SVM with a polynomial kernel achieved an accuracy of 96.77%, demonstrating its effectiveness in capturing the complex, non-linear patterns present in the data. The decision boundary produced by the polynomial kernel was sufficiently flexible to accommodate these patterns, leading to improved classification performance compared to a linear SVM. The use of a polynomial kernel in the SVM model allowed for the successful classification of data with non-linear relationships. The SVM with a polynomial kernel achieved a high accuracy of 96.77%, with strong precision and recall values for both categories. The F1-score of 0.95 for category R and 0.98 for category L highlights the model's ability to effectively classify the data with non-linear relationships, making it a superior choice compared to a linear SVM.

The SVM with an RBF kernel excelled in the classification task, achieving a remarkable accuracy of 98.06% on the test set. This performance surpasses that of models with linear and polynomial kernels, proving the suitability of the RBF kernel in managing complex data with non-linear relationships. The regularization parameter  $C=1$  was chosen after extensive experimentation to balance the trade-off between minimizing training error and avoiding overfitting. Higher  $C$  values ( $C > 1$ ) caused overfitting by overly penalizing misclassifications, while lower  $C$  values ( $C < 1$ ) led to underfitting by being too lenient. The kernel coefficient  $z=0.1$  was selected to allow each training point to have a broader influence, resulting in

smoother decision boundaries. Higher  $z$  ( $z > 0.1$ ) created overly complex boundaries, leading to overfitting, while lower  $z$  values ( $z < 0.1$ ) produced overly simplistic models that underfitted the data. The final configuration of  $C=1$  and  $z=0.1$  ( $z$  was determined through systematic trial and error, consistently delivering the highest accuracy and generalization across all tested configurations. The high precision and recall values across both categories demonstrate the model's reliability in accurately classifying data, while the F1-scores of 0.97 for category R and 0.99 for category L further emphasize its effectiveness in capturing intricate patterns. The RBF kernel's capacity to adapt to the underlying structure of the data allowed the SVM to deliver outstanding classification results, making it the most suitable choice for this task. The model's success in handling non-linear data distributions highlights the R-B-F kernel's flexibility and strong generalization capability, making it a robust option for a variety of classification challenges, especially those involving complex and non-linear feature relationships.

Table 1 presents the accuracy of different models used for the classification and prediction of Active-right or Active-left-nostril-breathing, and a cluster of accuracy comparisons is shown in Fig. 9. For every model, the performance measures, including recall, accuracy, and F1-score, are provided as shown in Table 2. The confusion matrices, precision-recall curve, and receiver operating characteristics (ROC) curve with area under the curve (AUC) values for SVM-linear, polynomial, and RBF kernel, KNN, and RF classifier that shown in Figs. 10-13 provide a clear and concise evaluation, offering transparency on the model's efficacy. From all the evaluation metrics, it is very evident that the SVM with RBF kernel model showed the highest prediction accuracy over Linear kernel and Polynomial kernel, and also over KNN and RF classifier. Hence, SVM with RBF kernel is chosen for prediction due to its robustness and an accuracy of 98.06% on the classification task.

Among the four models, the SVM-RBF kernel demonstrated the most significant performance. The model's performance was evaluated by making the predictions on the test sets, and the accuracy and confusion matrix obtained are presented in the result section. The trained SVM model with RBF kernel is saved to a file using pickle for future use.

### 3.5 Respiratory vitals

Using a customized algorithm, respiratory vitals were derived from the captured nasal parameter data. Using the cleaned data the respiratory vitals like Inhalation-time, exhalation-time, inter-breath intervals, breathing-rate, tidal volume and minute ventilation were acquired using the developed algorithm on an open source platform.

The temperature signals from the Active-right and Active-left-nostril groups were used to determine the respiratory vital characteristics, which are displayed in the bar graphs shown in Fig. 14, using the established method. It has been noted that the Active-right-nostril dominant group has shorter inter-

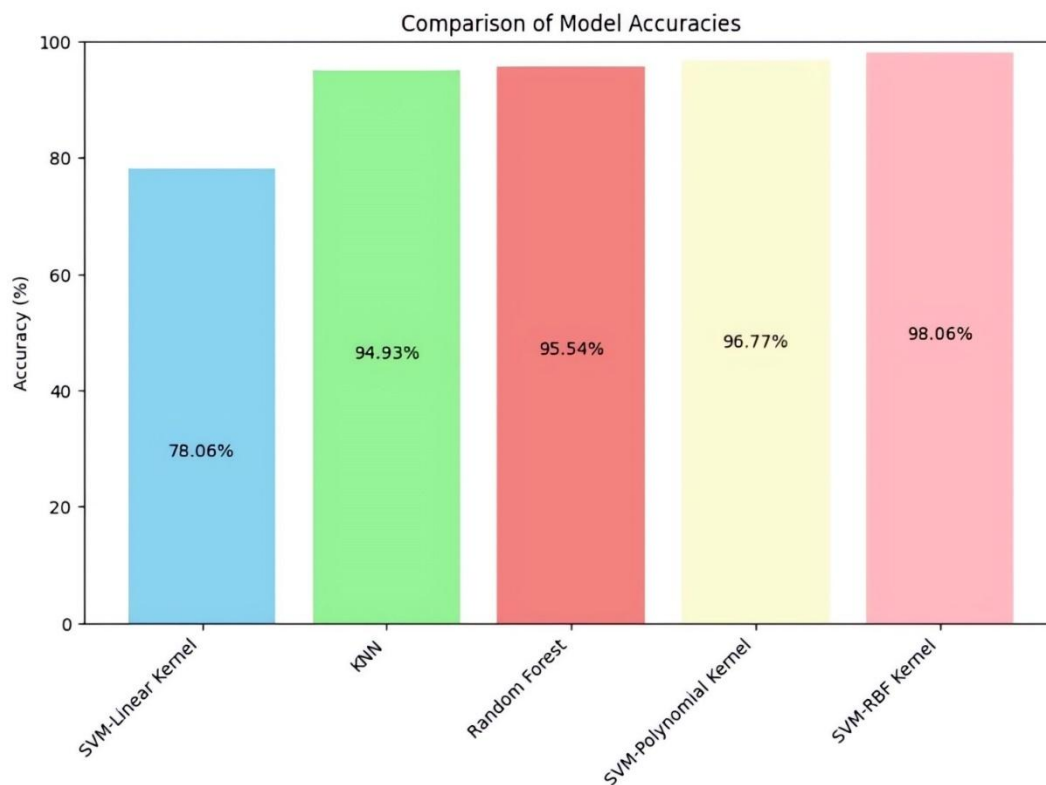


Fig. 9: Cluster of accuracy comparison using various models.

Table 1: Comparison of the accuracy of different models used for classification and prediction.

Model	Accuracy
SVM-linear kernel	78.6
KNN	95.0
RF	95.54
SVM polynomial kernel	96.77
SVM RBF kernel	98.06

Table 2: Performance Metrics of different models used for classification and prediction of Active-Right/Active-Left Nostril Breathing:

Model	Precision	Recall	F1-score
SVM-linear kernel	0.80	0.78	0.79
KNN	0.96	0.95	0.96
RF	0.96	0.95	0.96
SVM polynomial kernel	0.97	0.97	0.97
SVM RBF kernel	0.98	0.98	0.98

breath intervals, exhalation and inhalation times, indicating shorter times between breath cycles. This is further demonstrated by the fact that the Active-right-nostril group has greater values for breathing-rate, tidal volume, and minute ventilation than the Active-left-nostril-group. This suggests that higher breathing-rates and shorter inter-breath intervals in the Active-right-nostril group indicate stimulating sympathetic activity, whereas lower breathing rates in the Active-left-nostril group stimulated parasympathetic activity. This is connected to a person's physical and mental well-being.

### 3.6 Display of results

By harnessing technologies like Streamlit, Python, pickle, and

pandas synergistically, the frontend user interface of predicting active nostrils and displaying extracted features is developed. This offers a robust, user-friendly platform for users to interact with predictive models and obtain instantaneous insights into the type of breathing.

Screenshots of the web application presented in Fig. S1 offer a visual walkthrough of the interactive process. Given the input values containing temperature, pressure, and humidity values from the right and left nostrils from the Active-right-nostril-group considered for illustration, the web application presents the prediction results showing the final determination of the dominant nostril and displays all the respiratory vitals from right and left nostrils.

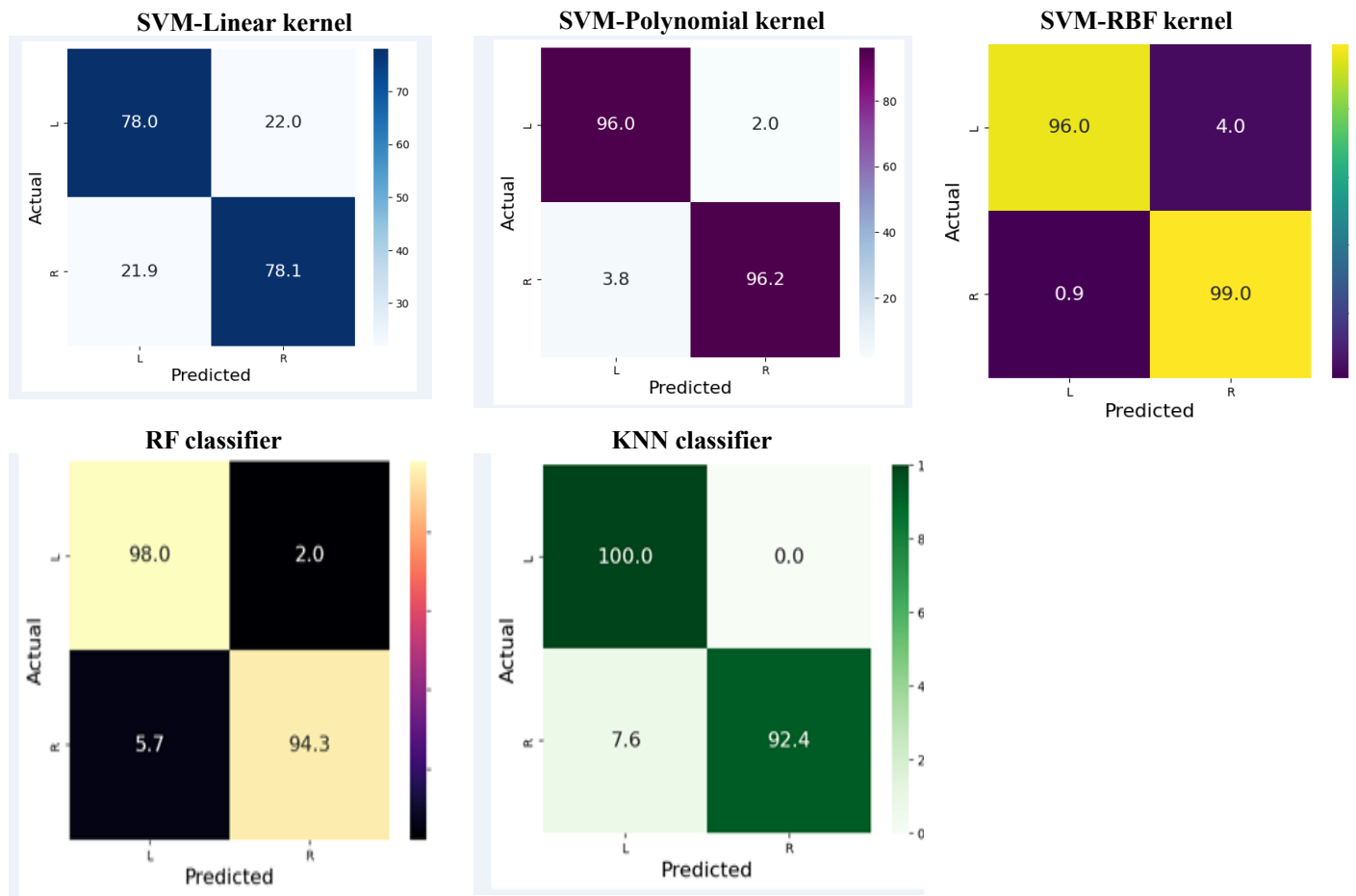


**Fig. 10:** Confusion matrices of various classification models for distinguishing between the active right nostril and active left nostril groups.

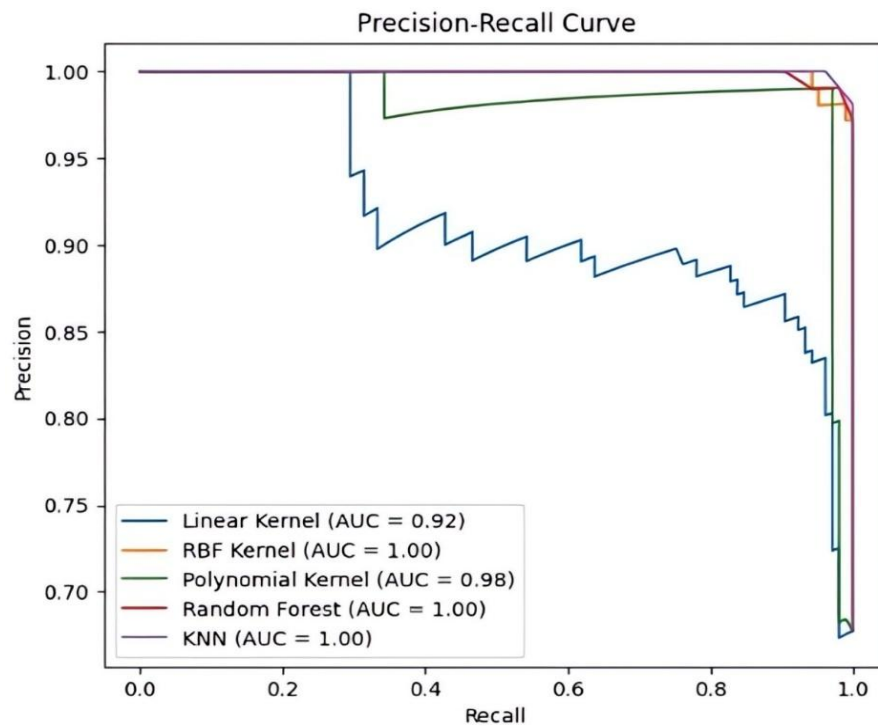


**Fig. 11:** Precision-recall curves of various classification models for distinguishing between the active right nostril and active left nostril groups.

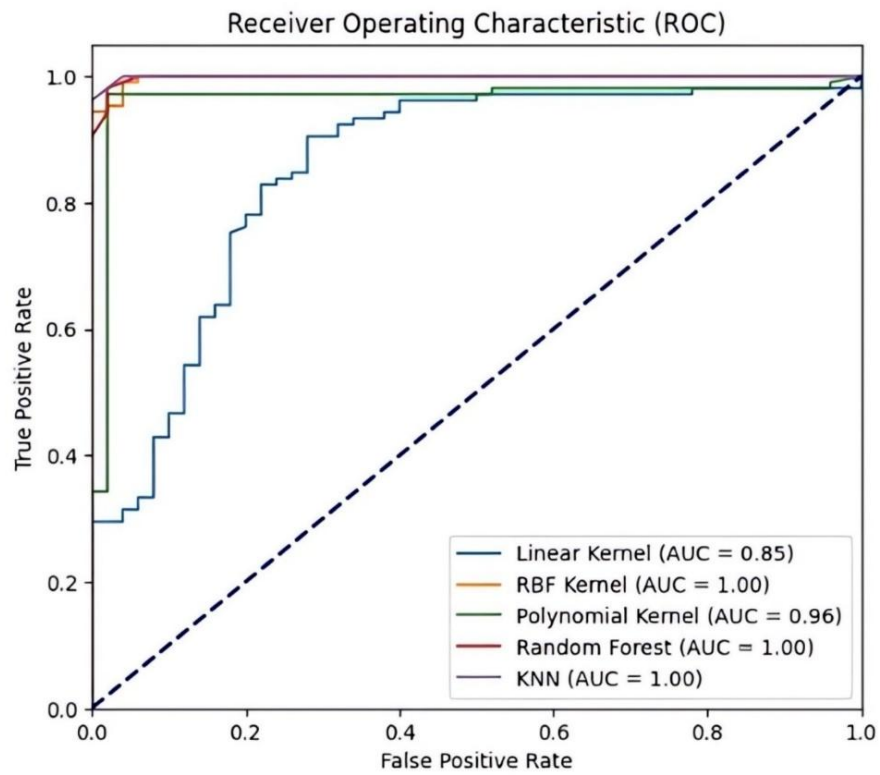


Fig. 12: ROC curves of various classification models for distinguishing between the active right nostril and active left nostril groups.

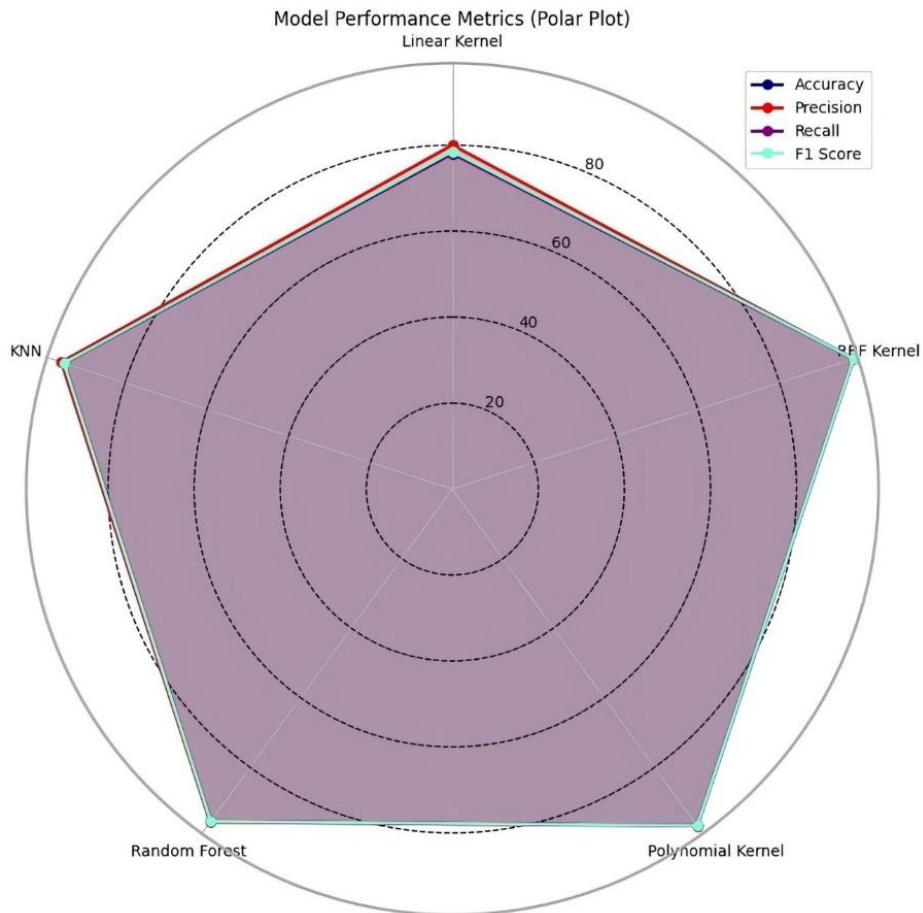
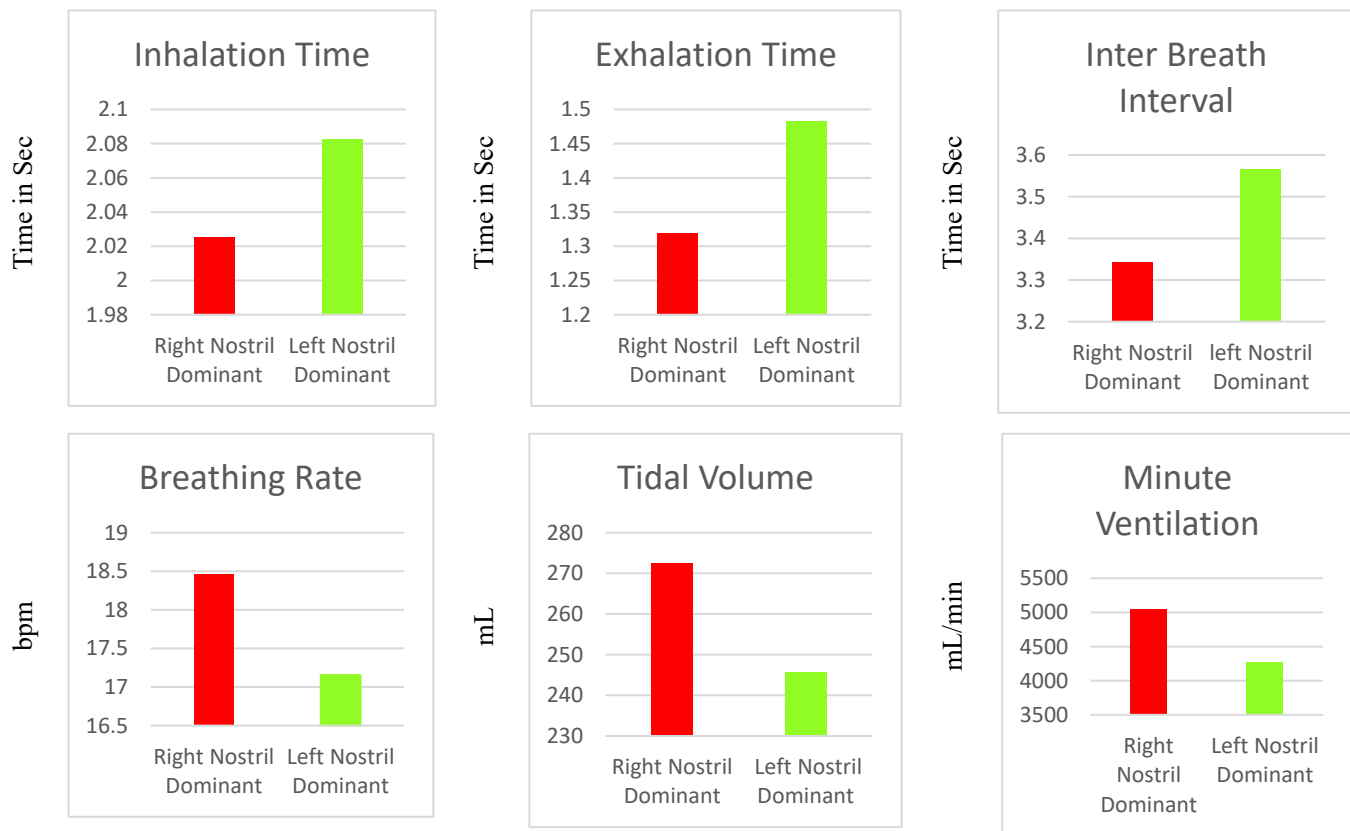


Fig. 13: Performance Metrics of different models used for classification and prediction of active-right/active left Nostril Breathing.



**Fig. 14:** Respiratory vitals among active right nostril and active left nostril groups extracted using breathing pattern taken out of temperature signals.

### 3.7 Discussion

The effect of having one nostril dominant over another nostril has a considerable impact on lung functions and also on cardiological function. It highlights the importance of sympathetic and parasympathetic nerves that innervate the airways and lungs. Individuals can be grouped as either right or left nasal dominance (RND) or (LND) based on how their nasal dominance affects their heart rate and pulmonary function measurements at rest. It's interesting to note that there is some evidence in the neuroscience literature supporting the idea that single-nostril breathing might alter autonomic function. Specifically, the right nostril tends to activate sympathetic effects, while the left nostril is more likely to produce relaxing effects. The descriptions of the parasympathetic and sympathetic nervous systems are very similar to the functions of the Ida and Pingala nadis when viewed through the lens of European-derived neuroscientific theory.<sup>[29]</sup> Heart Rate Variability indexes show an increase in parasympathetic activity in the left nostril breathing group and an increase in sympathetic activity in the right nostril breathing group.<sup>[30]</sup> During right nostril breathing, low frequency (LF), a marker of sympathetic activity, increases, high frequency (HF), a marker of parasympathetic activity, and their ratio, LF/HF, a marker of sympatho/vagal balance, decrease.<sup>[31]</sup> Therefore, using the right nostril to breathe raises sympathetic tone, which may be harmful to cardiovascular health.

Due to the significant decrease in systolic blood pressure (BP), diastolic BP, heart rate, and rate-pressure product following alternate nostril breathing exercise, its effects serve as a supplemental therapy for patients with hypertension.<sup>[32]</sup> Since left-nostril breathing (LNB) significantly lowers blood pressure and pulse rate, it can be utilized as a regular practice to help manage stress and strain from daily living.<sup>[33]</sup> Additionally, breathing via a specific nostril can change autonomic functions and metabolism because it increases sympathetic output to the adrenal medulla. Therefore, breathing via one nostril only has a noticeable calming or activating effect on the sympathetic nervous system, which may have therapeutic implications for changing metabolism.<sup>[34]</sup> As a result, the description of breathing patterns from individual nostrils is important because it provides information about how the respiratory and central neurological systems are related. Through this pilot study, we have attempted to analyze the breathing patterns of the right and left nostrils. The data set created at the Atamabodh Center for Learning and Healing, Bangalore, India, from yoga practitioners who are proficient in swara yoga practice, was grouped into active right nostril breathing and active left nostril breathing based on their response, as they are experts in checking their breathing status. This is analogous to nostril dominance, as the latter addresses the phenomenon where one nostril has a higher airflow than the other at any given time.

**Table 3** compares the cutting-edge methods that have been

**Table 3:** Different approaches for the characterization of active right and active left nostril breathings.

Ref. No.	Work done	Remarks
[15]	Using the temperature difference between inhale and exhale, analyzed the nasal cycle for different diseased conditions. A dominance in right nostril breathing was seen in conditions like peptic ulcer, eye diseases, hyper chloride, gastritis, diarrhea, insomnia, liver disorder, gastro intestinal disorder and cardiac diseases, where as people suffering from diseases like loss of appetite, tuberculosis, allergy, respiratory disorders like wheezing, and bronchitis asthma were breathing high in their left.	Temperature signals from right and left nostrils was acquired. Only manual assessment is performed without the implementation of any AI ML models.
[16]	Nasal pressure signals of long duration recordings were captured and assessed by developing a small portable device and characterized the nasal cycles using by deriving different numerical measures.	Characterization was performed using statistical analysis
[17]	The Cortical activity patterns were analyzed using the EEG signals during Right and left nostril breathing. Also using PSD of the EEG signals the effects of right and left nostril breathing was assessed.	Indirect measure of nostril dominance assessment.
[18]	Effects of nasal dominance on pulmonary function and heart rate parameters was assessed using a comparative analysis of parameters like oxygen saturation, pulse rate for different nostril breathing was performed using statistical analysis.	Signals are not directly captured from nostrils.
[30]	Assessed the effects of right nostril breathing (RNB) and left nostril breathing (LNB) on heart rate variability (HRV) and cardiovascular functions.	Indirect measure of nostril dominance assessment.
[31]	Effects of alternate nostril breathing and its effects on heart rate variability was analyzed. They performed the frequency domain analysis of HRV data.	Indirect measure of nostril dominance assessment. No implementation of AI-ML tools for assessment
[34]	The effect of different Pranayama procedures on nasal airflow signals were analyzed using statistical analysis.	Analysis using only statistical test i.e. no implementation of AI-ML tools for assessment
[35]	Developed a catheter system for the recording of nasal pressure signals from both nostrils and described an algorithm for processing and analyzing nasal pressure recordings using LabVIEW development environment.	Invasive set up for data acquisition AI-ML tools are not implemented

described in the suggested context and shows that numerous studies have used physiological signals, which are not exact measurements of the airflow signals from nostrils to characterize breathing and investigate the impact of active nostrils on human health.<sup>[35]</sup> Numerous papers have documented the consequences of breathing pattern on cardiovascular health in a clear manner, as the table indicates. The majority of breathing analyses are carried out by indirect measurements of respiratory signals, hence the creation of a setup that can record breathing signals from specific nostrils is necessary.

The recognition of Active nostrils during breathing has a potential impact, on various facets of human life studies, its exploration holds promise for shedding light on fundamental aspects of human behavior and health. Traditional methods of assessing individual nostril breathing have relied largely on subjective observation and rudimentary measurement

techniques. The crucial components of this work are the development of machine learning model to classify active-right nostril breathing and active-left nostril breathing, tasked with analyzing environmental data captured by nasal mask sensors to predict nostril dominance. Through data preprocessing and machine learning model training, the project achieved accurate prediction of nostril dominance (Active-right or Active-left) based on the sensed data. A user-friendly web application interface was created, allowing users to input environmental data, receive instantaneous predictions regarding nostril dominance, and display the respiratory vital parameters. The model's predictive capabilities may be constrained by the quantity and diversity of the training data. A larger and more diverse dataset could enhance generalization. Also, the system's performance may be influenced by variations in environmental conditions not fully represented in the training data. Thus, the challenges in the

current work include, achieving real-time predictions, especially when dealing with complex models, and the interpretability of the model's decisions, particularly in complex scenarios and also the creation of large data sets for analysis. This provides insight into areas for potential improvement and avenues for future work.

#### 4. Conclusion

With the successful development of a wearable nasal mask capable of capturing environmental variables such as temperature, humidity, and pressure from both nostrils, this work, aims to monitor nostril breathing using a unique method of physiological monitoring through the integration of wearable sensors and machine learning algorithms that marks a significant leap in wearable technology and healthcare. The computation of respiratory-vitals, such as breathing-rate (BR), inhalation-time (IT), exhalation-time (ET), inter-breath-interval (IBI), tidal-volume (TV), and minute-ventilation (MV), and the observation of their variation between active-right nostril breathing and active-left-nostril breathing, facilitates the improvement of personalized healthcare therapies and wellness monitoring. The classification of active-right-nostril and active-left-nostril breathing was successfully accomplished by SVM classifier using RBF kernel with an accuracy of 98 % compared to SVM using linear kernel and polynomial kernel, which had respective accuracies of 78.6% and 98.07%.

Additionally, it outperformed the KNN and Random forest classifiers with an accuracy of 95.54% and 95.0% for the categorization of the two-category breathing patterns that were taken into consideration. Because of the web application's user-centric design and user-friendly interface, which shows respiratory vital information and the type of breathing (active-right or active-left nostril breathing), people can better understand their physiological responses and make decisions about stress management, physical activity, and general well-being. Additionally, by evaluating the nature of breathing, the current work creates opportunities for future research in the fields of wearable technology, yoga, and healthcare innovation. This promotes interdisciplinary collaboration and advances the development of more approachable and efficient healthcare solutions. The current work's scope is always changing and growing, and it has the potential to influence outside of wearable technology by improving people's quality of life globally and driving advances in healthcare.

#### Acknowledgement

Authors would like to thank Mr. Sujan Nailady, Image Labels Pvt. Ltd, Bangalore, India and Rajkumar Dham, Founder Director, Atamabodh Centre for learning and healing, Bangalore India for their support towards executing this study. This study was supported by SERB-CII PM fellowship and RIT SEED FUNDING: 2020/RI5/R&D/IF/065. This work is also supported by the Technology Development Programme of IITI DRISHTI CPS Foundation under the National Mission

on Interdisciplinary Cyber Physical System (NM-ICPS) of the Department of Science and Technology, Government of India.

#### Conflict of Interest

There is no conflict of interest.

#### Supporting Information

Applicable.

#### References

- [1] I. N. Riga, Le syndrome neuro-réflexe de l'obstruction nasale unilatérale: note préliminaire / The neuro-reflex syndrome of unilateral nasal obstruction: preliminary note, *Revue D'otoneuro-Ophthalmologie*, 1957, **29**, 325-335.
- [2] G. Tillu, S. Chaturvedi, A. Chopra, B. Patwardhan, Public health approach of ayurveda and yoga for COVID-19 prophylaxis, *The Journal of Alternative and Complementary Medicine*, 2020, **26**, 360-364, doi: 10.1089/acm.2020.0129.
- [3] G. K. Pal, S. Velkumary, Madanmohan, Effect of short-term practice of breathing exercises on autonomic functions in normal human volunteers, *The Indian Journal of Medical Research*, 2004, **120**, 115-121.
- [4] Q. Li, G. Zheng, Y. Zheng, S. Wu, Influence of rhythmic breathing on immune function: A systematic review. *Chinese Journal of Integrative Medicine*, 2013, **19**, 722-730, doi: 10.1007/s11655-013-1603-1.
- [5] S. Rama, R. Ballentine, A. Hymes, Breathing and the nervous system, *The Science of Breath: A Practical Guide*. Himalayan Institute Press, Honesdale, PA, 1999, 123, ISBN: 9780893891510.
- [6] M. E. Vanutelli, C. Grigis, C. Lucchiari, Breathing right... or left! the effects of unilateral nostril breathing on psychological and cognitive wellbeing: a pilot study, *Brain Sciences*, 2024, **14**, 302, doi: 10.3390/brainsci14040302.
- [7] I. Homma, Y. Masaoka, Breathing rhythms and emotions, *Experimental Physiology*, 2008, **93**, 1011-1021, doi: 10.1113/expphysiol.2008.042424.
- [8] P. Yogananda, I. V. Chapter, Verse, *The Bhagavad Gita: Royal Science of God-Realization - The Immortal Dialogue Between Soul and Spirit, A New Translation and Commentary with Shiv Swarodaya and Arjuna, Self-Realization Fellowship*, Los Angeles, 2002, 496-507. ISBN: 9780876120309.
- [9] S. Telles, C. Joseph, S. Venkatesh, T. Desiraju, Alterations of auditory middle latency evoked potentials during yogic consciously regulated breathing and attentive state of mind, *International Journal of Psychophysiology*, 1993, **14**, 189-198, doi: 10.1016/0167-8760(93)90033-1.
- [10] P. Raghuraj, S. Telles, Immediate effect of specific nostril manipulating yoga breathing practices on autonomic and respiratory variables, *Applied Psychophysiology and Biofeedback*, 2008, **33**, 65-75, doi: 10.1007/s10484-008-9055-0.
- [11] P. S. Sarang, S. Telles, Oxygen consumption and respiration during and after two yoga relaxation techniques, *Applied Psychophysiology and Biofeedback*, 2006, **31**, 143-153, doi: 10.1007/s10484-006-9012-8.

- [12] A. Bhavanani, D. Pushpa, M. Ramanathan, R. Balaji, Differential effects of uninostil and alternate nostril pranayamas on cardiovascular parameters and reaction time, *International Journal of Yoga*, 2014, **7**, 60, doi: 10.4103/0973-6131.123489.
- [14] P. Raghuraj, S. Telles, Immediate effect of specific nostril manipulating yoga breathing practices on autonomic and respiratory variables, *Applied Psychophysiology and Biofeedback*, 2008, **33**, 65-75, doi: 10.1007/s10484-008-9055-0.
- [15] E. M. Kumaran, Alteration in nasal cycle rhythm as an index of the diseased condition, Pathophysiology - Altered Physiological States, InTechOpen, London, 2018, 1-13. ISBN: 9781789234269.
- [16] R. Kahana-Zweig, M. Geva-Sagiv, A. Weissbrod, L. Secundo, N. Soroker, N. Sobel, Measuring and characterizing the human nasal cycle, *PLoS One*, 2016, **11**, e0162918, doi: 10.1371/journal.pone.0162918.
- [17] I. K. Niazi, M. S. Navid, J. Bartley, D. Shepherd, M. Pedersen, G. Burns, D. Taylor, D. E. White, EEG signatures change during unilateral Yogi nasal breathing, *Scientific Reports*, 2022, **12**, 520, doi: 10.1038/s41598-021-04461-8.
- [18] S. Sinha, S. Mittal, S. Bhat, G. Baro, Effect of nasal dominance on pulmonary function test and heart rate, *International Journal of Yoga*, 2021, **14**, 141-145, doi: 10.4103/ijoy.ijoy-115-20.
- [19] D. Vitazkova, E. Foltan, H. Kosnacova, M. Micjan, M. Donoval, A. Kuzma, M. Kopani, E. Vavrinsky, Advances in respiratory monitoring: a comprehensive review of wearable and remote technologies, *Biosensors*, 2024, **14**, 90, doi: 10.3390/bios14020090.
- [20] M. Chu, T. Nguyen, V. Pandey, Y. Zhou, H. N. Pham, R. Bar-Yoseph, S. Radom-Aizik, R. Jain, D. M. Cooper, M. Khine, Respiration rate and volume measurements using wearable strain sensors, *NPJ Digital Medicine*, 2019, **2**, 8, doi: 10.1038/s41746-019-0083-3.
- [21] H. Cheraghi Bidsorkhi, N. Faramarzi, B. Ali, L. R. Ballam, A. G. D'Aloia, A. Tamburrano, M. S. Sarto, Wearable Graphene-based smart face mask for real-time human respiration monitoring, *Materials & Design*, 2023, **230**, 111970, doi: 10.1016/j.matdes.2023.111970.
- [22] C. Zhang, L. Zhang, Y. Tian, B. Bao, D. Li, A machine-learning-algorithm-assisted intelligent system for real-time wireless respiratory monitoring, *Applied Sciences*, 2023, **13**, 3885, doi: 10.3390/app13063885.
- [23] S. Muktibodhananda, Swara yoga in brief. In: Swara Yoga: The Tantric Science of Brain Breathing, Bihar School of Yoga, Munger, 1999, 1-12, ISBN: 9788185787121.
- [24] B. Yan, Z. Li, F. Zhou, X. Lv, F. Zhou, A fast sparse decomposition based on the teager energy operator in extraction of weak fault signals, *Sensors*, 2022, **22**, 7973, doi: 10.3390/s22207973.
- [25] T. Tao, C. Ji, C. Han, J. Wang, W. Sun, Study on the noise contents of different measurements in industrial process and their impact on process monitoring, *Computer Aided Chemical Engineering*, 2022, **51**, 1057-1062, doi: 10.1016/B978-0-323-95879-0.50177-6.
- [26] A. Chaudhary, S. Kolhe, R. Kamal, An improved random forest classifier for multi-class classification, *Information Processing in Agriculture*, 2016, **3**, 215-222, doi: 10.1016/j.inpa.2016.08.002.
- [27] L. Heutte, Keynote 3: Random forests for biomedical data classification, 2017 IEEE International Conference on Signal and Image Processing Applications, September 12-14, Kuching, Malaysia, IEEE, 2017, doi: 10.1109/icsipa.2017.8120567.
- [28] F. Pedregosa, G. Varoquaux, A. Gramfort, V. Michel, B. Thirion, O. Grisel, M. Blondel, P. Prettenhofer, R. Weiss, V. Dubourg, J. Vanderplas, A. Passos, D. Cournapeau, M. Brucher, M. Perrot, E. Duchesnay, G. Louppe, Scikit-learn: Machine learning in Python, *Journal of Machine Learning Research*, 2011, **12**, 2825-2830.
- [29] A. Venkatraman, R. Nandy, S. Rao, D. Mehta, A. Viswanathan, R. Jayasundar, Tantra and modern neurosciences: is there any correlation?, *Neurology India*, 2019, **67**, 1188, doi: 10.4103/0028-3886.271263.
- [30] G. Pal, A. Agarwal, S. Karthik, P. Pal, N. Nanda, Slow yogic breathing through right and left nostril influences sympathovagal balance, heart rate variability, and cardiovascular risks in young adults, *North American Journal of Medical Sciences*, 2014, **6**, 145, doi: 10.4103/1947-2714.128477.
- [31] R. K. Subramanian, Alternate nostril breathing at different rates and its influence on heart rate variability in non practitioners of yoga, *Journal of Clinical and Diagnostic Research*, 2016, **10**, 1-2, doi: 10.7860/jcdr/2016/15287.7094
- [32] M. J. Kumari, S. Kalaivani, G. K. Pal, Effect of alternate nostril breathing exercise on blood pressure, heart rate, and rate pressure product among patients with hypertension in JIPMER, Puducherry, *Journal of Education and Health Promotion*, 2019, **8**, 145, doi: 10.4103/jehp.jehp\_32\_19.
- [33] A. Naik, D. A. Biswas, S. Patel, Effect of left nostril breathing in hypertensives, *Journal of the Indian Academy of Clinical Medicine*, 2012, **13**, 15-17.
- [34] S. Telles, R. Nagarathna, H. R. Nagendra, Breathing through a particular nostril can alter metabolism and autonomic activities, *Indian Journal of Physiology and Pharmacology*, 1994, **38**, 133-137.
- [35] L. M. Umer, M. Kohler, K. E. Bloch, Automatic processing of nasal pressure recordings to derive continuous side-selective nasal airflow and conductance, *Frontiers in Physiology*, 2019, **9**, 1814, doi: 10.3389/fphys.2018.01814.

**Publisher's Note:** Engineered Science Publisher remains neutral with regard to jurisdictional claims in published maps and institutional affiliations.

#### Open Access

This article is licensed under a Creative Commons Attribution 4.0 International License, which permits the use, sharing, adaptation, distribution and reproduction in any medium or format, as long as appropriate credit to the original author(s) and the source is given by providing a link to the Creative

Commons license and changes need to be indicated if there are any. The images or other third-party material in this article are included in the article's Creative Commons license, unless indicated otherwise in a credit line to the material. If material is not included in the article's Creative Commons license and your intended use is not permitted by statutory regulation or exceeds the permitted use, you will need to obtain permission directly from the copyright holder. To view a copy of this license, visit <http://creativecommons.org/licenses/by/4.0/>.

©The Author(s) 2025